

An Adaptive Fuzzy Sliding-Mode Controller Design for Walking Control with Functional Electrical Stimulation: A Computer Simulation Study

Vahab Nekoukar, and Abbas Erfanian

Abstract: A major challenge to developing neuroprostheses for walking and to widespread acceptance of these walking systems is the design of a robust control strategy that provides satisfactory tracking performance, to be robust against time-varying properties of *neuromusculoskeletal* dynamics, day-to-day variations, muscle fatigue, and external disturbances, and to be easy to apply without requiring offline identification during different experiment sessions. The lower extremities of human walking are a highly nonlinear, highly time-varying, multi-actuator, multi-segment with highly inter-segment coupling, and inherently unstable system. Moreover, there always exist severe structured and unstructured uncertainties such as spasticity, muscle fatigue, external disturbances, and unmodeled dynamics. Robust control design for such nonlinear uncertain multi-input multi-output system still remains as an open problem. In this paper we present a novel robust control strategy that is based on combination of adaptive fuzzy control with a *new* well-defined sliding-mode control (SMC) with strong reachability for control of walking in paraplegic subjects. Based on the universal approximation theorem, fuzzy logic systems are employed to approximate the *neuromusculoskeletal* dynamics and an adaptive fuzzy controller is designed by using Lyapunov stability theory to compensate for approximation errors. The proposed control strategy has been evaluated on a planar model of bipedal locomotion as a virtual patient. The results indicate that the proposed strategy provides accurate tracking control with fast convergence during different conditions of operation, and could generate control signals to compensate the effects of muscle fatigue, system parameter variations, and external disturbances. Interesting observation is that the controller generates muscle excitation that mimic those observed during normal walking.

Keywords: Functional electrical stimulation (FES), sliding-mode control (SMC), adaptive, fuzzy logic.

1. INTRODUCTION

For over three decades, many research groups have shown that limited crutch- or walker-assisted walking can be restored in subjects with spinal cord injuries by means of functional neuromuscular stimulation (FNS) systems [1]. These systems are open-loop systems in which the stimulation parameters are prescribed open-loop through a trial-and-error process. In FNS systems, sequences of current pulses excite the intact peripheral axon, which in turn contract paralyzed muscles. By changing the pulse width, pulse amplitude, or the pulse frequency, the level of contraction can be altered to perform a specific task. To provide functional use of the paralyzed limbs, an appropriate electrical stimulation pattern should be delivered to a set of muscles.

A major impediment to stimulating the paralyzed

neuromuscular systems and determining the stimulation pattern has been the highly non-linear, time-varying properties of electrically stimulated muscle, muscle fatigue, spasticity, and day-to-day variations which limit the utility of pre-specified stimulation patterns and open-loop FNS control systems.

To deal with these problems, many control strategies have been developed and reported in literature including fixed-parameter feedback controller [2], [3], adaptive feedback techniques [4]-[7], fixed-parameter feedforward [8], [9], adaptive feedforward [9]-[14], and combination of feedforward and feedback control techniques [8], [9], [10], [15]. However, despite a great deal of research in this area, only a few studies have been devoted to closed-loop control of walking with functional electrical stimulation [16]-[18]. Popović *et al.* [16], Anderson and Panty [17], and Thelen and Anderson [18] used optimal control method to determine the muscle activations that, when input into a forward dynamic musculoskeletal model, produce the desired trajectory of human walking. The model used by Popović *et al.* consisted of one leg and trunk. The leg was modeled as a planar, two segmental linkage of rigid bodies. The model of musculoskeletal was reduced to a double pendulum with a moving hanging point which interfaces with the rest of the body and the ground. The double pendulum representing the leg allowed knee and hip extension and flexion within physiological limits.

Manuscript received ???; revised ???; accepted ???.

Vahab Nekoukar and Abbas Erfanian are with the Department of Biomedical Engineering, Iran Neural Technology Research Centre, Iran University of Science and Technology (IUST), Tehran, Iran (e-mail: nekoukar@iust.ac.ir, erfanian@iust.ac.ir).

The leg was driven by two pairs of monoarticular muscles acting around the hip and knee joints and did not include active ankle and phalangeal joints. The *neuromusculoskeletal models of the body used by Anderson and panty [16] and Thelen and Anderson [17]* to simulate normal walking on level ground are more complicated models with more details. *The body was modeled as an 8-segment with a 21-degree-of-freedom articulated linkage actuated by 92 Hill-type muscle-tendon units [17].*

Optimal control is not suitable for online control of walking. It can be used for offline analysis of excitation patterns required to produce a trajectory and estimation of the contribution of muscles to movement. To implement the optimal control for walking, an accurate model of *multilink neuromusculoskeletal* system is required. Due to time-varying property of *neuromusculoskeletal* system, subject-to-subject variations, un-modeled dynamics, model uncertainties, and disturbances, determining the muscle activation patterns using optimal control is much less efficient for online control of walking in paraplegic subjects.

An effective approach to deal with the uncertainties is adaptive control. Adaptive control, by online tuning the parameters (of either the plant or the controller—corresponding to indirect, or direct adaptive control), can deal with uncertainties, but generally, suffers from the disadvantage of being able to achieve only *asymptotical* convergence of the tracking error to zero. Several issues, such as transient performance, un-modeled dynamics, disturbance, the amount of offline training required, the tradeoff between the persistent excitation of signals for correct identification and the steady system response for control performance, the model convergence and system stability issues in real applications, and nonlinearity in parameters, often complicate the adaptive approach [19]-[22].

A useful and powerful control scheme to deal with the uncertainties, nonlinearities, and bounded external disturbances is the sliding mode control (SMC) [23]. In robust control designs, a fixed control law based on *a priori* information on the uncertainties is designed to compensate for their effects, and *exponential* convergence (finite time) of the tracking error to a (small) ball centered at the origin is obtained. Robust control has some advantages over the adaptive control, such as its ability to deal with disturbances, quickly varying parameters, and un-modeled dynamics [23]. Nevertheless, the SMC suffers from the high frequency oscillations in the control input, which called "chattering" [24], [25]. The chattering caused by high-frequency switching control activity is highly undesirable because it leads to low control accuracy and may excite un-modeled high frequency plant dynamics which could result in unpredictable instability [24].

In previous work [26], we designed a control methodology which is based on synergistic combination of two artificial neural networks with sliding mode control (SMC) for control of knee-joint angle with quadriceps muscle stimulation. Although the controller

provides excellent tracking performance with no chattering for single muscle group stimulation, the online computation burden to update the parameters of neural networks is not appropriate for multi-actuator and multi-joint movement. In [27], we presented a robust control strategy resulting in a simpler design for control of the ankle-joint angle with stimulation of ankle dorsiflexor and plantarflexor muscles. However, both controllers are based on offline identification of the muscle-joint dynamics. This causes the method to be impractical for online control of human walking. Due to the inherent instability of human walking, identification of its model is very difficult.

In this paper, we present a novel robust control system that is based on SMC and fuzzy logic system, referred to as *adaptive fuzzy sliding mode control* (AFSMC), for online control of walking, while the dynamics of walking is identified online without requiring any offline calibration. This new controller takes advantages of the fast dynamic behavior (i.e., strong sliding reachability) and robustness of the sliding mode control while does not require any offline identification of the plant being controlled.

2. PROBLEM STATEMENT

Sliding mode control is one of the effective nonlinear robust control approaches since it provides system dynamics with an invariance property to uncertainties and external disturbances provided matching conditions are satisfied. To implement the SMC, the plant being controlled should be first presented in a standard canonical form. Identification of the canonical model for multiple-input multiple-output (MIMO) nonlinear systems, and in particular for inherently unstable systems is very difficult and very different from those for SISO systems.

In this paper, based on the universal approximation theorem [28], the fuzzy logic system is used to approximate the unknown multiple-input multiple-output (MIMO) nonlinear system (i.e., neuromusculoskeletal system) and designed adaptive laws based on Lyapunov stability theory for *online* updating the model parameters.

In recent years, based on the universal approximation theorem, there has been much research on the design of sliding-mode controller based on fuzzy logic system for unknown single-input-single-output (SISO) nonlinear systems [29]–[32], single-input-multiple-output (SIMO) nonlinear systems [33], and MIMO nonlinear systems [34]–[39]. Zheng *et al.* [36] proposed a fuzzy SMC based on Takagi–Sugeno fuzzy system for control of MIMO nonlinear systems. The basic idea in this approach is first to decompose the nonlinear dynamic system into N fuzzy-based linear state-space subsystems in the form: $\dot{\mathbf{x}} = \mathbf{A}_i \mathbf{x}(t) + \mathbf{B}_i \mathbf{u}(t)$, where $\mathbf{x}(t) \in \mathbb{R}^n$ is the vector of state variables, $\mathbf{u}(t) \in \mathbb{R}^m$ is the vector of control inputs; and \mathbf{A}_i and \mathbf{B}_i are constant matrices. Next, the overall fuzzy model is achieved by fuzzy aggregation of each individual model. However, the assumptions which are

made on linear subsystems limit the application of the method to plants that are complex and ill-defined. Hwang [39] has also introduced a Takagi–Sugeno based adaptive fuzzy SMC. To track a trajectory dominant by a specific frequency, the reference linear models with desired amplitude and phase features were established by the same fuzzy sets of the system rule. However, the main difficulty with this approach is the establishing a set of reference linear models for a physical nonlinear dynamical system (e.g., *neuromusculoskeletal* system). To improve the reaching dynamics during reaching phase of SMC, Tong and Li [37] proposed a fuzzy adaptive SMC by choosing a strong sliding reachability condition. To implement the SMC, the MIMO nonlinear system should be presented in *controllability canonical* form $\mathbf{y}^{(n)} = \mathbf{f}(\mathbf{x}) + \mathbf{g}(\mathbf{x}) \cdot \mathbf{u}$, where \mathbf{x} is the overall state vector, $\mathbf{u} \in \mathbb{R}^p$ the control input vector, $\mathbf{y} \in \mathbb{R}^p$ the system output vector, $\mathbf{f}(\mathbf{x}) \in \mathbb{R}^p$ and $\mathbf{g}(\mathbf{x}) \in \mathbb{R}^{p \times p}$ are unknown nonlinear continuous functions. To meet control objectives in sliding mode, it is required that $\mathbf{g}(\mathbf{x})$ to be regular. Since the nonlinear functions $\mathbf{f}(\mathbf{x})$ and $\mathbf{g}(\mathbf{x})$ are unknown, Tong and Li [37] used two fuzzy systems $\hat{\mathbf{f}}(\mathbf{x}, \boldsymbol{\theta}_f)$ and $\hat{\mathbf{g}}(\mathbf{x}, \boldsymbol{\theta}_g)$, to approximate the nonlinear functions $\mathbf{f}(\mathbf{x})$ and $\mathbf{g}(\mathbf{x})$ respectively. $\boldsymbol{\theta}_f$ and $\boldsymbol{\theta}_g$, are the adjustable parameters of the approximations. One can notice that the above controller is not well-defined if $\hat{\mathbf{g}}(\mathbf{x}, \boldsymbol{\theta}_g)$, is not regular.

All the above mentioned works [29], [30], [36], [37], [38] do not guarantee the estimate $\hat{\mathbf{g}}(\mathbf{x}, \boldsymbol{\theta}_g)$, to be regular. To solve the controller regularity problem, we use the method proposed in [40], to develop a *new* well-defined SMC with strong sliding reachability.

3. CONTROL DESIGN

3.1. Sliding mode control with strong sliding reachability

Consider the following MIMO nonlinear systems represented by

$$\mathbf{x}^{(n)} = \mathbf{F}(\mathbf{x}) + \mathbf{G}(\mathbf{x}) \cdot \mathbf{u} \quad (1)$$

where $\mathbf{x} = [x_1, \dots, x_1^{(n_1-1)}, \dots, x_m, \dots, x_m^{(n_m-1)}]^T \in \mathbb{R}^m$ is a vector of states which are assumed to be measurable, $\mathbf{u} = [u_1, \dots, u_m]^T \in \mathbb{R}^m$, is the control input vector, $\mathbf{F}(\mathbf{x})$ and $\mathbf{G}(\mathbf{x})$ are unknown nonlinear but continuous functions defined as

$$\mathbf{F}(\mathbf{x}) = [f_1(\mathbf{x}), \dots, f_m(\mathbf{x})]^T$$

$$\mathbf{G}(\mathbf{x}) = \begin{bmatrix} g_{11}(\mathbf{x}) & \cdots & g_{1m}(\mathbf{x}) \\ \vdots & & \vdots \\ g_{m1}(\mathbf{x}) & \cdots & g_{mm}(\mathbf{x}) \end{bmatrix}$$

Assumption 1. The matrix $\mathbf{G}(\mathbf{x})$ is positive definite, then it exists $\delta_0 > 0, \delta_0 \in \mathbb{R}$ such that: $\mathbf{G}(\mathbf{x}) \geq \delta_0 \mathbf{I}_m$.

Assumption 2. The desired trajectory $x_{di}(t)$, $i = 1, \dots, m$, is a known bounded function of time

with bounded known derivatives and $x_{di}(t)$ is assumed to be n_i -times differentiable.

To implement SMC, the sliding surface is defined as

$$s_i(t) = \left(\frac{d}{dt} + \lambda_i \right)^{n_i-1} e_i(t), \quad i = 1, \dots, m \quad (2)$$

where $e_i(t) = x_{di}(t) - x_i(t)$. Using (1), differentiation of (2) with respect to time can be written as

$$\dot{\mathbf{s}} = \mathbf{v} - \mathbf{F}(\mathbf{x}) - \mathbf{G}(\mathbf{x}) \cdot \mathbf{u} \quad (3)$$

where $\dot{\mathbf{s}} = [\dot{s}_1(t), \dots, \dot{s}_m(t)]$ and $\mathbf{v} = [v_1, \dots, v_m]$ with each variable v_i defined as

$$v_1 = x_{d1}^{(n_1)} + \beta_{1,n_1} e_1^{(n_1-1)} + \dots + \beta_{1,1} e_1$$

$$\dots$$

$$v_m = x_{dm}^{(n_m)} + \beta_{m,n_m} e_m^{(n_m-1)} + \dots + \beta_{m,1} e_m \quad (4)$$

with

$$\beta_{i,k} = \frac{(n_i-1)!}{(n_i-k)!(k-1)!} \lambda_i^{n_i-k}, \quad i = 1, \dots, m, \quad k = 1, \dots, n_i-1 \quad (5)$$

A strong sliding reachability condition is defined as [41]:

$$\dot{\mathbf{s}}(t) = -\mathbf{K}_0 \mathbf{s}(t) - \mathbf{K}_1 \text{sgn}(\mathbf{s}) \quad (6)$$

with \mathbf{K}_0 being a positive-definite matrix,

$$\mathbf{K}_1 = \text{diag}(k_{11}, \dots, k_{1m}) > 0, \quad \text{and} \quad \text{sgn}(\mathbf{s}) = [\text{sgn}(s_1), \dots, \text{sgn}(s_m)]^T.$$

It should be noted that this kind of reachability will force $\mathbf{s}(t) \rightarrow 0$ exponentially or in finite time. Therefore, $e_i(t)$ and all its derivatives up to n_i-1 converges to zero exponentially or in finite time. By virtue of (3) and (6), the equivalent control law can be obtained as:

$$\mathbf{u}_{eq} = \mathbf{G}^{-1}(\mathbf{x}) (-\mathbf{F}(\mathbf{x}) + \mathbf{v} + \mathbf{K}_0 \mathbf{s} + \mathbf{K}_1 \text{sgn}(\mathbf{s})). \quad (7)$$

Due to the fact that system functions $\mathbf{F}(\mathbf{x})$ and $\mathbf{G}(\mathbf{x})$ are unknown in practical systems, the control law (7) is usually difficult to be obtained. Here, we use fuzzy logic system to approximate the nonlinear unknown functions and design an adaptive fuzzy controller by using Lyapunov stability theory to compensate for approximation errors.

3.2. Adaptive Fuzzy Sliding Mode Control

Based on the universal approximation theorem [26], fuzzy logic systems can be used to approximate the vector functions $\mathbf{F}(\mathbf{x})$ and the matrix function $\mathbf{G}(\mathbf{x})$ in (7). Let $\hat{\mathbf{F}}(\mathbf{x}, \boldsymbol{\theta}_f)$ and $\hat{\mathbf{G}}(\mathbf{x}, \boldsymbol{\theta}_g)$ be the fuzzy approximation of the vector functions $\mathbf{F}(\mathbf{x})$ and the matrix function $\mathbf{G}(\mathbf{x})$ in (7), respectively. So, (7) can be written as

$$\mathbf{u}_{eq} = \hat{\mathbf{G}}^{-1}(\mathbf{x}, \boldsymbol{\theta}_g) (-\hat{\mathbf{F}}(\mathbf{x}, \boldsymbol{\theta}_f) + \mathbf{v} + \mathbf{K}_0 \mathbf{s} + \mathbf{K}_1 \text{sgn}(\mathbf{s})) \quad (8)$$

There is a major problem in using (8) as an equivalent control law when matrix $\hat{\mathbf{G}}(\mathbf{x}, \boldsymbol{\theta}_g)$ is singular. There is no guarantee that $\hat{\mathbf{G}}(\mathbf{x}, \boldsymbol{\theta}_g)$ remains regular during estimating. To solve this problem, we use the regularized inverse of $\hat{\mathbf{G}}(\mathbf{x}, \boldsymbol{\theta}_g)$ defined as [40]

$$\hat{\mathbf{G}}^{-1}(\mathbf{x}, \boldsymbol{\theta}_g) = \hat{\mathbf{G}}^T(\mathbf{x}, \boldsymbol{\theta}_g) [\varepsilon_0 \mathbf{I}_m + \hat{\mathbf{G}}(\mathbf{x}, \boldsymbol{\theta}_g) \hat{\mathbf{G}}^T(\mathbf{x}, \boldsymbol{\theta}_g)]^{-1} \quad (9)$$

where ε_0 is a small positive constant and \mathbf{I}_m is $m \times m$ identity matrix. The regularized inverse (9) is well-defined even when $\hat{\mathbf{G}}(\mathbf{x}, \boldsymbol{\theta}_g)$ is singular, and therefore the control law defined in (10) is always well-defined.

$$\mathbf{u}_{eq} = \hat{\mathbf{G}}^T(\mathbf{x}, \boldsymbol{\theta}_g) [\varepsilon_0 \mathbf{I}_m + \hat{\mathbf{G}}(\mathbf{x}, \boldsymbol{\theta}_g) \hat{\mathbf{G}}^T(\mathbf{x}, \boldsymbol{\theta}_g)]^{-1} \quad (10)$$

$$\left(-\hat{\mathbf{F}}(\mathbf{x}, \boldsymbol{\theta}_f) + \mathbf{v} + \mathbf{K}_0 \mathbf{s} + \mathbf{K}_1 \text{sgn}(\mathbf{s}) \right)$$

Fuzzy Approximator

To implement the SMC (10), the nonlinear functions $\mathbf{F}(\mathbf{x})$ and $\mathbf{G}(\mathbf{x})$ should be estimated. In this work, we use $m(m+1)$ fuzzy systems to approximate these nonlinear functions. The fuzzy system uses the fuzzy IF-THEN rules to perform a mapping from an input vector $\mathbf{x} = [x_1, x_2, \dots, x_n]^T \in \mathbb{R}^n$ to an output $y \in \mathbb{R}$. The r th fuzzy rule is written as

R^r : if x_1 is $A_1^r(x_1)$ and...and x_n is $A_n^r(x_n)$, then y is B^r where A_i^r and B^r are fuzzy sets with membership functions $\mu_{A_i^r}(x_i)$ and $\mu_{B^r}(y)$, respectively, and \mathbf{x} belongs to a compact set. By using the product-inference rule, singleton fuzzifier, and center-average defuzzifier, the output of FLS can be expressed as

$$y = \frac{\sum_{i=1}^{n_r} \tilde{y}^i \left(\prod_{j=1}^n \mu_{A_j^i}(x_j) \right)}{\sum_{i=1}^{n_r} \left(\prod_{j=1}^n \mu_{A_j^i}(x_j) \right)} = \boldsymbol{\theta}^T \boldsymbol{\psi}(\mathbf{x}) \quad (11)$$

where n_r is the number of total fuzzy rules, \tilde{y}^i is the point at which $\mu_{B^i}(\tilde{y}^i) = 1$, $\mu_{A_j^i}(x_j)$ is the membership function of the fuzzy variable x_j characterized by Gaussian function, $\boldsymbol{\theta} = [\tilde{y}^1, \tilde{y}^2, \dots, \tilde{y}^{n_r}]^T$ is an adjustable parameter vector, and $\boldsymbol{\psi} = [\psi^1, \psi^2, \dots, \psi^{n_r}]^T$ is a fuzzy basis vector, where ψ^i is defined as

$$\psi^i(\mathbf{x}) = \frac{\left(\prod_{j=1}^n \mu_{A_j^i}(x_j) \right)}{\sum_{i=1}^{n_r} \left(\prod_{j=1}^n \mu_{A_j^i}(x_j) \right)} \quad (12)$$

By using the introduced fuzzy systems in (11), approximation of functions $f_i(\mathbf{x})$ and $g_{ik}(\mathbf{x})$ can be obtained as follows:

$$\hat{f}_i(\mathbf{x}) = \boldsymbol{\theta}_{f_i}^T \boldsymbol{\psi}_{f_i}(\mathbf{x}), \quad i = 1, \dots, m \quad (13)$$

$$\hat{g}_{ik}(\mathbf{x}) = \boldsymbol{\theta}_{g_{ik}}^T \boldsymbol{\psi}_{g_{ik}}(\mathbf{x}), \quad i, k = 1, \dots, m \quad (14)$$

where $\boldsymbol{\theta}_{f_i}(\mathbf{x})$ and $\boldsymbol{\theta}_{g_{ik}}(\mathbf{x})$ are adjustable parameter

vectors. There are optimal parameters $\boldsymbol{\theta}_{f_i}^*$ and $\boldsymbol{\theta}_{g_{ik}}^*$ such that:

$$\boldsymbol{\theta}_{f_i}^* = \arg \min_{\boldsymbol{\theta}_{f_i}} \left\{ \sup_{\mathbf{x} \in D_x} |f_i(\mathbf{x}) - \hat{f}_i(\mathbf{x}, \boldsymbol{\theta}_{f_i})| \right\} \quad (15)$$

$$\boldsymbol{\theta}_{g_{ik}}^* = \arg \min_{\boldsymbol{\theta}_{g_{ik}}} \left\{ \sup_{\mathbf{x} \in D_x} |g_{ik}(\mathbf{x}) - \hat{g}_{ik}(\mathbf{x}, \boldsymbol{\theta}_{g_{ik}})| \right\} \quad (16)$$

Now we can define minimum estimation errors as:

$$\boldsymbol{\varepsilon}_f = \mathbf{F}(\mathbf{x}) - \hat{\mathbf{F}}(\mathbf{x}, \boldsymbol{\theta}_f^*) \quad (17)$$

$$\boldsymbol{\varepsilon}_g = \mathbf{G}(\mathbf{x}) - \hat{\mathbf{G}}(\mathbf{x}, \boldsymbol{\theta}_g^*) \quad (18)$$

We assumed that minimum estimation errors are bounded for all $\mathbf{x} \in D_x$:

$$|\boldsymbol{\varepsilon}_f(\mathbf{x})| \leq \bar{\varepsilon}_f, \quad |\boldsymbol{\varepsilon}_g(\mathbf{x})| \leq \bar{\varepsilon}_g, \quad \forall \mathbf{x} \in D_x \quad (19)$$

that $\bar{\varepsilon}_f$ and $\bar{\varepsilon}_g$ are positive constant.

Adaptation Laws

To approximate the uncertain nonlinear functions $f_i(\mathbf{x})$ and $g_{ik}(\mathbf{x})$ in (1), adaptive update laws to adjust the parameter vectors in (13) and (14) need to be developed. The update laws are chosen as

$$\dot{\boldsymbol{\theta}}_{f_i} = -\eta_{f_i} \boldsymbol{\psi}_{f_i}(\mathbf{x}) s_i \quad (20)$$

$$\dot{\boldsymbol{\theta}}_{g_{ik}} = -\eta_{g_{ik}} \boldsymbol{\psi}_{g_{ik}}(\mathbf{x}) s_i u_{eqk} \quad (21)$$

where $\eta_{f_i} > 0$ and $\eta_{g_{ik}} > 0$.

Also, a corrective controller is defined to guarantee the stability of the closed-loop control system and compensate the approximation errors. Under assumptions 1 and 2, a control input is chosen as

$$\mathbf{u} = \mathbf{u}_{eq} + \mathbf{u}_c \quad (22)$$

where \mathbf{u}_{eq} is given in (10), and \mathbf{u}_c is defined as

$$\mathbf{u}_c = \frac{\mathbf{s}^T \left(\bar{\varepsilon}_f + \bar{\varepsilon}_g \|\mathbf{u}_{eq}\| + \|\mathbf{u}_0\| \right)}{\delta_0 \|\mathbf{s}\|^2} \quad (23)$$

$$\mathbf{u}_0 = \varepsilon_0 [\varepsilon_0 \mathbf{I}_m + \hat{\mathbf{G}}(\mathbf{x}) \hat{\mathbf{G}}^T(\mathbf{x})]^{-1} \quad (24)$$

$$\left(-\hat{\mathbf{F}}(\mathbf{x}) + \mathbf{v} + \mathbf{K}_0 \mathbf{s} + \mathbf{K}_1 \text{sgn}(\mathbf{s}) \right)$$

Theorem 1: Consider the MIMO system (1) with nonlinear functions $\mathbf{F}(\mathbf{x})$ and $\mathbf{G}(\mathbf{x})$ which are approximated by (13) and (14). Suppose that assumptions 1 and 2 are satisfied, the control input is chosen as (22), and adaptation laws are selected as (20) and (21). Then,

- All signals in the closed-loop system are bounded.
- The tracking errors and their derivatives decrease asymptotically to zero.

Proof: Given in Appendix A.

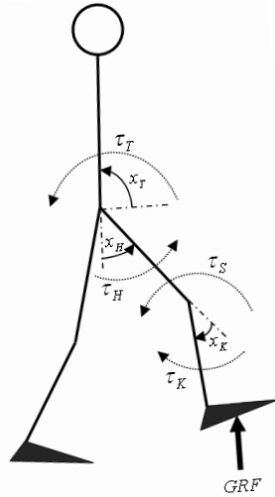


Fig. 1. Model of the body showing the definition of angles and torques considered.

4. MODEL OF HUMAN WALKING

A planar model of bipedal locomotion [16] is considered here as a virtual patient. The leg is modeled as a planar, two segmental linkage of rigid bodies as thigh and shank. It is assumed that the leg is driven by two pairs of monoarticular muscles acting around the hip and knee joints (Fig. 1). Ankle and phalangeal joints are not included in the model because it is assumed that the subject will wear ankle-foot orthoses during the walking. The head, arms, and torso are lumped into a single rigid body as the upper extremity. The upper body and one leg are replaced by the torque contributing to the total torques applied at the hip joint and knee joint of the second leg. The interaction between the foot and the floor is modelled as a rigid contact and the effects of ground reaction are included at the base. We treated ground reaction forces as inputs to the simulation. Thus, the model simulated here is reduced to a double pendulum with a moving hanging point which interfaces with the rest of the body and the ground. Further details were described in [16].

The following describes the equation of motion of the musculoskeletal system:

$$\mathbf{M}\ddot{\mathbf{x}}(t) + \mathbf{C}\dot{\mathbf{x}}(t) + \mathbf{G} + \boldsymbol{\tau}_{fd} = \boldsymbol{\tau}(t) + \mathbf{v}(t) \quad (25)$$

where $\mathbf{x}(t) = [x_K \ x_H]^T$ and $\dot{\mathbf{x}}(t) = [\dot{x}_K \ \dot{x}_H]^T$ are the vector of generalized coordinates and velocities (i.e., joint angles, angular velocities), respectively; $\mathbf{M}: \mathbf{R}^2 \rightarrow \mathbf{R}^{2 \times 2}$ is the inertia matrix, $\mathbf{C}: \mathbf{R}^2 \times \mathbf{R}^2 \rightarrow \mathbf{R}^{2 \times 2}$ is the generalized coriolis and centrifugal matrix, $\mathbf{G}: \mathbf{R}^2 \rightarrow \mathbf{R}^2$ is a vector of gravity, $\boldsymbol{\tau}_{fd} = [\tau_{fdS} \ \tau_{fdT}]^T$ is a vector of ground reaction torque and torque that is produced by the upper extremity weight, $\mathbf{v}(t)$ is a white-noise process presenting the lumped time-varying process uncertainty, and $\boldsymbol{\tau}(t) = [\tau_S \ \tau_K]^T$ is a vector of torques acting at the shank and thigh segments defined by

$$\begin{aligned} \tau_i(t) &= \tau_i^f(t) - \tau_i^e(t) - \tau_i^r(t) \quad i = K, H \\ \tau_T(t) &= -\tau_K(t) \\ \tau_S(t) &= \tau_K(t) + \tau_H(t) \end{aligned} \quad (26)$$

where $\tau_i^f(t)$ and $\tau_i^e(t)$ are the flexor and extensor torques, respectively, $\tau_i^r(t)$ is the resistive torque produced by passive tissues crossing the joints, and $\tau_i(t)$ is the torque acting at the hip and knee joints. The model of electrically stimulated muscle used in this study included the neural activation dynamics and multiplicative nonlinear torque-angle and torque-velocity scaling factors [16], [42] as

$$\tau_i^j = (c_{i2}^j x_i^2 + c_{i1}^j x_i + c_{i0}^j) \cdot g_i^j(\dot{x}_i) \cdot a_i^j \quad i = K, H; \quad j = f, e \quad (27)$$

where x_K and x_H are the knee and hip joint angles, respectively. The angles x_{K0} and x_{H0} are the neutral positions where the moments are zero. The second order polynomial in (27) represents the relationships between joint angle and joint torque. The normalized joint torques versus joint angular velocities are determined by [16]:

$$g_i^f(\dot{x}_i) = \begin{cases} b_{i1} & \dot{x}_i < \frac{1-b_{i1}}{b_{i2}} \\ 1-b_{i2}\dot{x}_i & \frac{1-b_{i1}}{b_{i2}} \leq \dot{x}_i < \frac{1}{b_{i2}} \\ 0 & \frac{1}{b_{i2}} \leq \dot{x}_i \end{cases}$$

$$g_i^e(\dot{x}_i) = \begin{cases} 0 & \dot{x}_i < \frac{-1}{b_{i3}} \\ 1+b_{i3}\dot{x}_i & \frac{-1}{b_{i3}} \leq \dot{x}_i < \frac{b_{i4}-1}{b_{i3}} \\ b_{i4} & \frac{b_{i4}-1}{b_{i3}} \leq \dot{x}_i \end{cases} \quad (28)$$

The variables a_i^j are the activation of the extensor and flexor muscles and given by [42]:

$$\dot{a}_i^j(t) = \begin{cases} (u_i^j(t) - a_i^j(t)) / \tau_{act} + (1 - u_i^j(t)) / \tau_{deact}, & u_i^j(t) \geq a_i^j(t) \\ (u_i^j(t) - a_i^j(t)) / \tau_{deact}, & u_i^j(t) < a_i^j(t) \end{cases} \quad (29)$$

where the parameters τ_{act} and τ_{deact} are time constants for activation and deactivation, respectively. The values of 20 and 60 ms were adopted for activation and deactivation, respectively. The variables u_i^j are the normalized levels of stimulation for the muscles. The resistive torques, $\tau_i^r(t)$, are given by [16]:

$$\begin{aligned} \tau_K^r &= d_{11}(x_K - x_{K0}) + d_{12}\dot{x}_K + d_{13}e^{d_{14}x_K} - d_{15}e^{d_{16}x_K} \\ \tau_H^r &= d_{21}(x_H - x_{H0}) + d_{22}\dot{x}_H + d_{23}e^{d_{24}x_H} - d_{25}e^{d_{26}x_H} \end{aligned} \quad (30)$$

All of the muscles flexing the joint are represented as a single flexor muscle, and all of the muscles extending the joint as a single extensor muscle. Further details were described in [16], [42]-[44].

The set of parameters c_{ik}^j ($k=0,1,2$), b_{ik} ($k=1,2,3,4$), and d_{ik} ($k=1,\dots,6$) are taken from [16], [42]. The lumped process uncertainty, $\mathbf{v}(t)$, is generated by passing a white noise with zero mean and variance σ^2 through a

Butterworth lowpass digital filter with a cutoff frequency of $\omega_c = 5$ Hz. The standard deviation was selected to be $\pm 20\%$ of the peak torque generated at the joint.

The aim of controller is to determine the levels of muscle stimulation to generate desired movement despite of system parameter variations, external disturbances and muscle fatigue.

5. RESULTS

The reference trajectories of the torso, hip, and knee joint angles during walking and the ground reaction forces were obtained from an experiment with a able-bodied subject (male, $H = 176$ cm, $M = 58$ kg). Different walking trials were conducted each with about 10 strikes. To avoid transient effects, the measured data during the first three strides and the last two strides were not considered for simulation. The joint angles were measured by using the motion tracker system MTx (Xsens Technologies, B.V.) which is a small and accurate 3DOF Orientation Tracker. The ground reaction forces were recorded by pedar-x system (novel) which is an accurate and reliable pressure distribution measuring system for monitoring local loads between the foot and the shoe. The data were recorded at 100 Hz. The hip acceleration was calculated by using the kinematic data.

The mean absolute error (MAE) was calculated as a measure of tracking accuracy as follows:

$$\bar{e}_K = \frac{1}{n} \sum_{j=1}^n |x_K(j) - x_K^d(j)|, \quad \bar{e}_H = \frac{1}{n} \sum_{j=1}^n |x_H(j) - x_H^d(j)|, \quad \bar{e} = (\bar{e}_K + \bar{e}_H)/2$$

where n is the number of samples, x_K^d and x_H^d are the desired values of knee and hip joint angles, respectively.

The control objective is to design a control law to force the system state variables (i.e., joint angles x_K and x_H) to track the desired state trajectories x_K^d and x_H^d in the presence of model uncertainties, external disturbances, and time-varying properties of the *neuromusculoskeletal* system.

The average of total muscle activities (ATMA) was calculated to measure the energy expenditure as follows:

$$\text{ATMA} = \left(\frac{1}{4T} \sum_{t=1}^T (a_K^f(t) + a_K^e(t) + a_H^f(t) + a_H^e(t)) \right) \times 100,$$

where a_i represents the muscle activity of each muscle and T is the duration of walking simulation (i.e., five strides).

The system described by (25) is used as a virtual patient. To implement the AFSMC, the musculoskeletal system should be presented in a standard canonical form as:

$$\ddot{\mathbf{x}} = \mathbf{F}(\mathbf{x}) + \mathbf{G}(\mathbf{x}) \cdot \mathbf{u}$$

where $\mathbf{x} = [x_K \dot{x}_K x_H \dot{x}_H]^T$ are vector of joint angles and angular velocities and $\mathbf{u}(t) = [u_K u_H]^T$ is the control

outputs of the hip and knee joints. Control of flexor and extensor muscles across each joint is accomplished by switching the stimulation signal between two muscle groups as

$$u_i^{\text{flexor}}(t) = \begin{cases} u_i(t) & \text{if } u_i(t) > 0 \\ 0 & \text{otherwise} \end{cases}$$

$$u_i^{\text{extensor}}(t) = \begin{cases} 0 & \text{if } u_i(t) > 0 \\ -u_i(t) & \text{otherwise} \end{cases} \quad i = K, H$$

The system functions $\mathbf{F}(\mathbf{x})$ and $\mathbf{G}(\mathbf{x})$ are unknown and estimated online by fuzzy logic system presented in 3.2 without any offline calibration. The controller parameters are chosen heuristically to achieve the best controller performance during simulation studies. In this study, we choose parameters of the proposed controller as the following:

$$\eta_{f_i} = \eta_{g_{ik}} = 0.45, \quad \varepsilon_0 = 0.1, \quad \bar{e}_{f_i} = \bar{e}_{g_{ik}} = 0, \quad \delta_0 = 0.6,$$

$$\lambda_i = 38, \quad k_{0i} = 10, \quad k_{1i} = 185, \quad \theta_{f_i}(0) = \theta_{g_{ik}}(0) = 0.1, \text{ for } i, k = 1, 2.$$

5.1. Trajectory tracking

Fig. 2(a) shows the results of the adaptive fuzzy sliding mode control of walking in a virtual subject. It is observed that excellent tracking performance can be achieved with acceptable switching activity in the control input. Interesting observation is the fast convergence of the proposed control strategy. The joint angle trajectories converge to the desired trajectory after about 200 ms. *It should be noted that the values of model parameters (1) is identified online without any offline identification and offline calibration.*

The values of MAE are $\bar{e}_K = 0.90^\circ \pm 0.74^\circ$, $\bar{e}_H = 0.81^\circ \pm 0.51^\circ$, $\bar{e} = 0.85^\circ$. The maximum values of absolute error are $\bar{e}_{K_{\max}} = 4.85^\circ$, $\bar{e}_{H_{\max}} = 2.44^\circ$. The tracking errors obtained here are comparable with the results obtained using optimal control used in [16] when the weighting factor¹ λ set to 0 (Table 1). However, the ATMA obtained by using proposed AFSMC is about 14.65% which is 30.24% less than that obtained by the optimal control. Increasing the weighting factor reduces the agonist and antagonist activations but increases the tracking errors. It is observed that by setting λ to 0.001, the performance of optimal control has degraded, MAE increases to 5.76° , and ATMA decreases to 15.44% (Table 1). In this case, the maximum of the absolute error on hip joint is 24.79° which may cause falling and high energy consumption during walking.

¹In [24], a cost function was selected as the sum of the squares of the tracking errors from the desired trajectories, and the weighted sum of the squares of agonist and antagonist activations of the muscle groups acting around the hip and knee joints (see [24]). The λ is the weight factor of the sum of the squares of muscle groups activations.

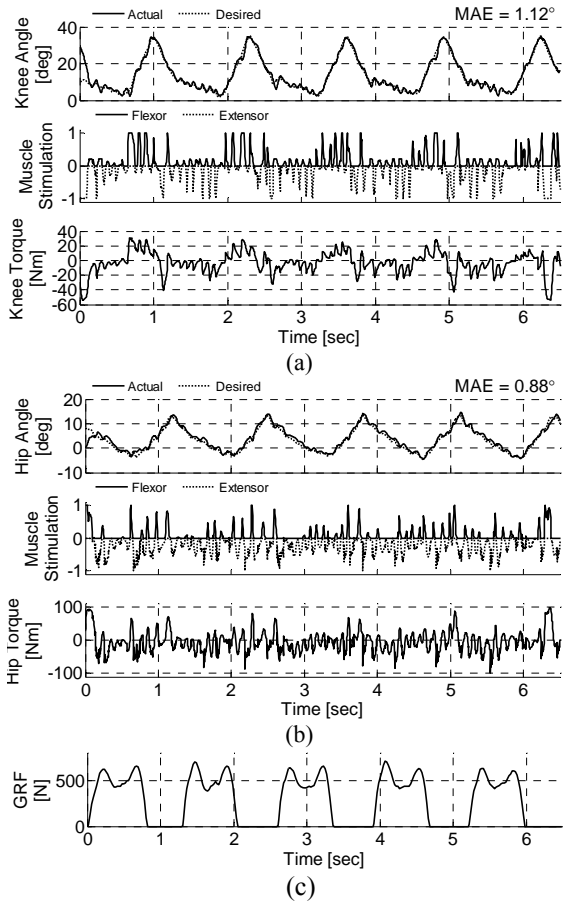


Fig. 2. Results of the human walking control using the proposed AFSMC: Measured (desired) and actual joint angle, stimulation signals of flexor and extensor muscle groups, and the net torque acting at the shank and thigh. (a) Knee joint. (b) Hip joint. (c) Ground reaction force.

It should be noted that the optimal control proposed in [16] should be determined under the condition $v(t) = 0$. In this case, the optimal controller fails to track the desired trajectories.

Fig. 3 shows the average of walking control results over the five gait cycles. It is observed that during loading response, between heel strike and opposite toe off, the knee and hip extensors were activated to extend the joints. The knee was flexed a little at the initial of loading response by activation of the knee flexor. The knee flexion during loading response contributed to shock absorption. During mid stance, the first half of single limb support (between 14% and 30% of gait cycle), both the hip and knee were extended by activation of both joint extensors. During terminal stance, the second half of single limb support, the knee increased its extension, and began to flex slightly at the end of this phase.

During pre-swing phase, between 47% and 61% of gait cycle, it is observed that the knee flexor was activated. The torque acting at the shank was positive which was a flexor moment. During initial swing, between opposite heel-strike and toe-off, the limb responded with greater knee flexion by activating the knee flexor and loss of hip extension by activating the hip flexor. During initial swing which is initiated at the time the toe loses contact with the floor, sufficient knee flexion is critical for proper toe clearance during swing.

Table 1. Mmean absolute tracking error (\pm Standard deviation), Maximum absolute tracking error and ATMA obtained using the proposed adaptive fuzzy sliding mode controller and the optimal controller [24].

Method	Conditions	\bar{e}_K	\bar{e}_H	\bar{e}_{mean}	$\bar{e}_{K\ max}$	$\bar{e}_{H\ max}$	ATMA		
AFSMC	$v(t) \neq 0$	Fixed-parameter	$0.90^\circ \pm 0.74^\circ$	$0.81^\circ \pm 0.51^\circ$	0.85°	4.85°	2.44°	14.65%	
		External Disturbance	$1.02^\circ \pm 0.87^\circ$	$0.95^\circ \pm 0.60^\circ$	0.99°	6.96°	2.82°	15.83%	
		Time-varying parameter	$1.35^\circ \pm 1.17^\circ$	$1.60^\circ \pm 1.46^\circ$	1.47°	6.86°	7.08°	21.91%	
		Fatigue	$1.03^\circ \pm 0.92^\circ$	$1.02^\circ \pm 0.66^\circ$	1.02°	6.97°	4.61°	24.09%	
Optimal	$v(t) = 0$	$\lambda = 0$	Fixed-parameter	$0.65^\circ \pm 0.59^\circ$	$0.54^\circ \pm 0.33^\circ$	0.60°	3.46°	2.23°	44.89%
			Time-varying parameter	$3.24^\circ \pm 2.98^\circ$	$14.32^\circ \pm 10.03^\circ$	8.78°	24.55°	41.12°	54.99%
		$\lambda = 0.001$	Fixed-parameter	$3.74^\circ \pm 2.49^\circ$	$7.78^\circ \pm 6.25^\circ$	5.76°	8.21°	24.79°	15.44%
			Time-varying parameter	$6.57^\circ \pm 6.12^\circ$	$17.00^\circ \pm 13.25^\circ$	11.79°	27.33°	42.47°	17.15%

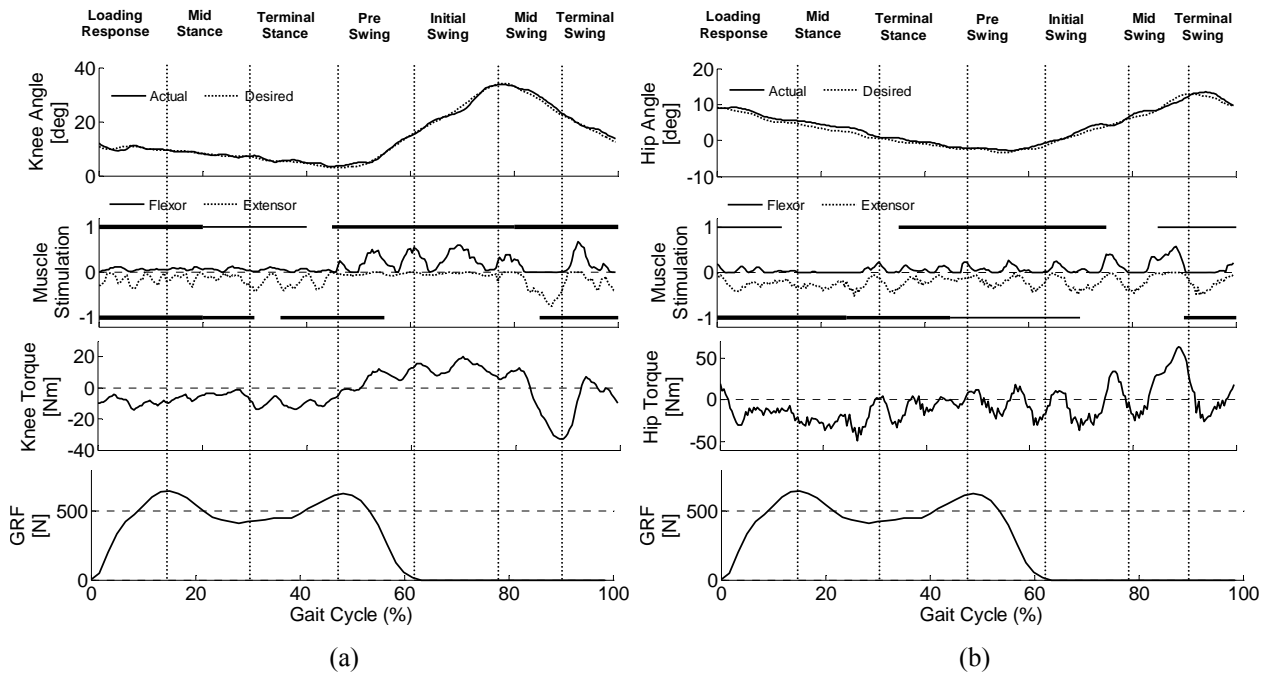


Fig. 3. Average of walking control results over five gait cycles: Measured (desired) and actual joint angle, stimulation signals of flexor and extensor muscle groups, torque acting at the joint and the net torque acting at the shank and thigh. (a) Knee joint. (b) Hip joint. (c) Average ground reaction force. The EMG activities (horizontal black bars) were obtained by averaging the results reported in the literature [52], [54].

During mid swing (between 78% and 90% of gait cycle), the knee flexor was deactivated and its extensor was activated to extend the knee while the hip flexor was activated to increase its flexion and to advance the limb. The knee and hip flexors and hip extensor work synergistically to flex the hip from an extend position during swing phases. During terminal swing (between 90% and 100% of gait cycle), the knee increased its extension and the hip began its extension by activation of the hip extensor.

A comparison of these muscle excitation patterns to EMG data reported by others during normal walking is shown in Fig. 3 [44], [46]. The muscle excitation patterns generated by the controller were, for the most part, consistent with EMG data.

5.2. Effects of External Disturbances

To evaluate the ability of proposed control strategy to external disturbance rejection, a constant torque in amount of 150 Nm (which is about 200% of maximum generated torque acting at the thigh segment during disturbance-free trial) was applied to the thigh in posterior and anterior directions, at 1.3 s and at 3.75 s, respectively, each time for a period of 1.2 s. Anterior and posterior disturbances were imposed at the thigh by adding and subtracting a constant torque in amount of 150 Nm to and from the torque acting at the hip, respectively.

Fig. 4 shows the results of disturbance rejection. It is observed that during posterior disturbance, the activity of the hip extensor was decreased but its flexor activity was increased. Posterior disturbance causes not only hip

extension but also knee extension, thus the knee flexor activity was increased to reject the posterior disturbance. During anterior disturbance which has been applied to the thigh during mid swing, activities of the knee extensor and hip flexor have been decreased but activities of the knee flexor and hip extensor have been increased. It is observed that during anterior disturbance the activity of hip extensor has been saturated and thus tracking error has been increased.

The MAE was calculated for the whole sequence of walking (five consecutive strides). The results show that the values of MAE are $\bar{e}_K = 1.02^\circ \pm 0.87^\circ$, $\bar{e}_H = 0.95^\circ \pm 0.60^\circ$, $\bar{e} = 0.99^\circ$. Comparing the results with that of obtained during simulated walking without disturbances, we see that a robust tracking performance and fast convergence can be achieved under external disturbances using proposed AFSMC. The maximum values of absolute error are $\bar{e}_{K \max} = 6.96^\circ$, $\bar{e}_{H \max} = 2.82^\circ$.

5.3. Effects of System Parameter Variations

To evaluate the performance of controller under system parameter variations, all muscle parameters c_{ik} ($i=1, \dots, 4; k=0, \dots, 4$) and d_{ik} ($i=1, 2; k=0, \dots, 6$) were randomly varied $\pm 80\%$ from their nominal values. Table 1 summarizes the values of MAE and the maximum values of absolute error over the five consecutive strides. It is observed that the values of MAE are $\bar{e}_K = 1.35^\circ \pm 1.17^\circ$, $\bar{e}_H = 1.60^\circ \pm 1.46^\circ$.

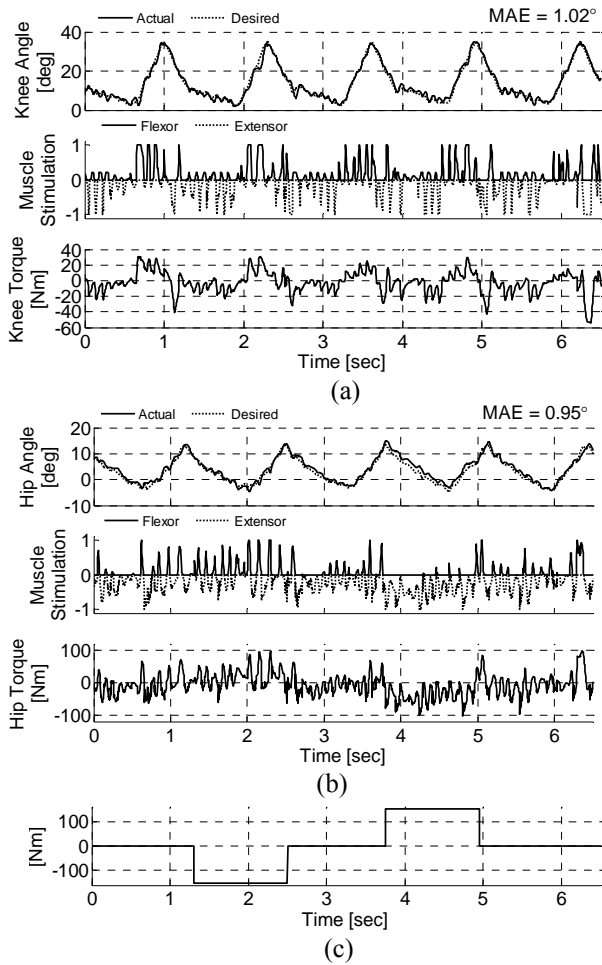


Fig. 4. Results of external disturbance rejection obtained using the proposed AFSMC: Measured (desired) and actual joint angle, stimulation signals of flexor and extensor muscle groups, and the torque acting at the joint. (a) Knee joint. (b) Hip joint. (c) External disturbance profile which was applied to the hip in posterior and anterior directions at 1.3 s and at 3.75 s, respectively.

The average of MAE is 1.47° during time-varying condition while it is 0.85° during fixed-parameter condition. The results indicate that the proposed control strategy is robust against system parameter variations. This interesting result indicates that the proposed control strategy can be used for different experiment sessions on different days and different subjects without any offline calibration of the controller and can compensate the time-varying properties of neuromuscular dynamics. It is observed that during time-varying condition, the performance of optimal control is significantly degraded (average of MAE is 8.78°).

5.4. Effects of Muscle Fatigue

To evaluate the ability of the controller to account for muscle fatigue, the effects of muscle fatigue were simulated by an asymptotic decrease in the agonist's (antagonist's) muscle gain to 50% of its original value

over 120 s. The ability of the controller to continuously adjust the stimulation pattern to achieve consistent tracking performance is demonstrated in Fig. 5. This plot shows the 25 strides of walking (i.e., 32.5 s). The recorded data from consecutive experimental trials were concatenated to obtain a long distance walking. It is observed that the stimulation patterns (Fig. 5) were adapted to produce the desired output torque trajectory from beginning of simulation. Fig. 5 demonstrates that the proposed AFSMC can also provide a very good tracking performance during muscle fatigue ($\bar{e}_K = 1.03^\circ \pm 0.92^\circ$, $\bar{e}_H = 1.02^\circ \pm 0.66^\circ$, $\bar{e} = 1.02^\circ$).

6. DISCUSSION AND CONCLUSION

In this paper, a novel robust control strategy incorporating the SMC with strong reachability condition and adaptive fuzzy control has been proposed for control of human walking. In this design, an adaptive law was derived based on Lyapunov stability analysis for online adapting the parameters of the model so that closed-loop stability and asymptotic convergence to zero of tracking errors and its derivatives can be guaranteed.

The current controllers for FES applications (e.g., joint control and walking) require offline identification before they could be used to control the limbs (e.g., see [16]-[18], [26], [27]). The burdens of offline identification may hinder the clinical applications of motor neuroprostheses. A major contribution of the current study is that the proposed control scheme does not require offline calibration or offline identification. The adaptation of the model is performed online without requiring any offline adjustment of model parameters.

Simulation studies on a virtual patient demonstrated the exceptional performance and robustness of the proposed control system against system parameter variations, muscle fatigue, external disturbances, and unmodeled dynamics. The results show that the average of MAE is 0.85° which is nearly equal to tracking error obtained by the optimal control proposed in [16] with $\lambda = 0$. However, the average muscle groups activations obtained by optimal control is 44.89% which is 30.24% higher than that obtained by proposed AFSMC.

The most prominent property of the proposed AFSMC is its insensitivity to the plant parameter variations. However, it is observed that the performance of optimal control is significantly degraded during parameter variations. The MAE increases substantially to 8.78° and the maximum absolute error are $\bar{e}_{K \max} = 24.55^\circ$, $\bar{e}_{H \max} = 41.12^\circ$.

Another important feature of the proposed method is that the state trajectories can be controlled to achieve the fast convergence. The knee and hip movement trajectories converge to the desired trajectories after about 200 ms. The fast convergence is the direct consequence of the strong reachability condition of the proposed control strategy.

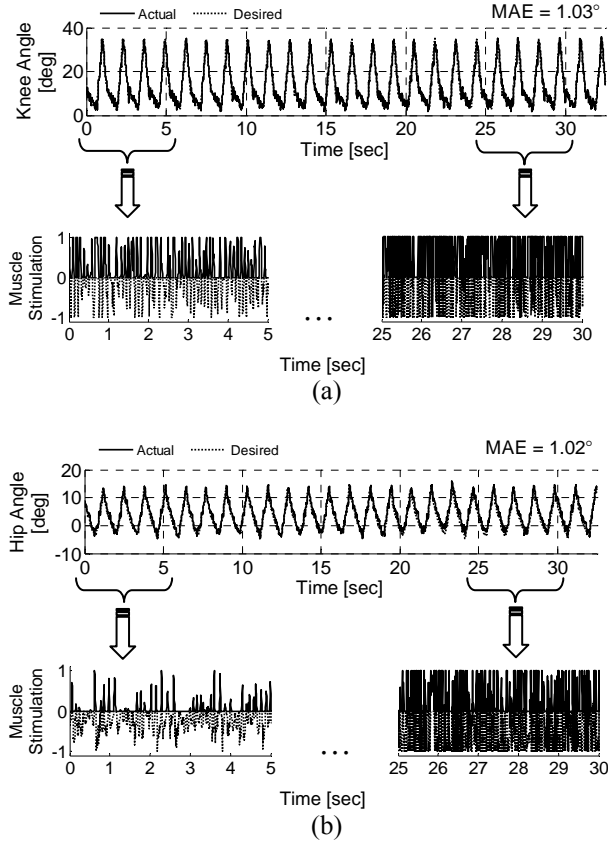


Fig. 5. Results of fatigue compensation obtained using proposed AFSMC: Measured (desired) and actual joint angle, stimulation signals of flexor and extensor muscle groups. (a) Knee joint. (b) Hip joint.

Future work will consider the exploitation of this strategy for the control of walking in paraplegic subjects that are active participants in a rehabilitation research program involving daily electrically stimulated exercise of their lower limbs (either seated or during standing and walking) using ParaWalk neuroprosthesis [45].

APPENDIX A

Proof of Theorem 1: Consider the following Lyapunov function candidate:

$$V = \frac{1}{2} \mathbf{s}^T \mathbf{s} + \frac{1}{2} \sum_{i=1}^m \frac{1}{\mu_{f_i}} \tilde{\theta}_{f_i}^T \tilde{\theta}_{f_i} + \frac{1}{2} \sum_{i=1}^m \sum_{k=1}^m \frac{1}{\mu_{g_{ik}}} \tilde{\theta}_{g_{ik}}^T \tilde{\theta}_{g_{ik}} \quad (\text{A1})$$

The time derivative of V is

$$\dot{V} = \mathbf{s}^T \dot{\mathbf{s}} - \sum_{i=1}^m \frac{1}{\mu_{f_i}} \tilde{\theta}_{f_i}^T \dot{\tilde{\theta}}_{f_i} - \sum_{i=1}^m \sum_{k=1}^m \frac{1}{\mu_{g_{ik}}} \tilde{\theta}_{g_{ik}}^T \dot{\tilde{\theta}}_{g_{ik}} \quad (\text{A2})$$

Substituting (22) into (3), we have

$$\dot{\mathbf{s}} = \mathbf{v} - \mathbf{F}(\mathbf{x}) - (\mathbf{G}(\mathbf{x}) - \hat{\mathbf{G}}(\mathbf{x})) \mathbf{u}_{eq} - \hat{\mathbf{G}}(\mathbf{x}) \mathbf{u}_{eq} - \mathbf{G}(\mathbf{x}) \mathbf{u}_c \quad (\text{A3})$$

From (22)-(24) and the fact

$$\hat{\mathbf{G}}(\mathbf{x}) \hat{\mathbf{G}}^T(\mathbf{x}) [\varepsilon_0 \mathbf{I}_m + \hat{\mathbf{G}}(\mathbf{x}) \hat{\mathbf{G}}^T(\mathbf{x})]^{-1} = \mathbf{I}_m - \varepsilon_0 [\varepsilon_0 \mathbf{I}_m + \hat{\mathbf{G}}(\mathbf{x}) \hat{\mathbf{G}}^T(\mathbf{x})]^{-1}$$

we have

$$\dot{\mathbf{s}} = -\mathbf{K}_0 \mathbf{s} - \mathbf{K}_1 \text{sgn}(\mathbf{s}) - (\mathbf{F}(\mathbf{x}) - \hat{\mathbf{F}}(\mathbf{x})) - (\mathbf{G}(\mathbf{x}) - \hat{\mathbf{G}}(\mathbf{x})) \mathbf{u}_{eq} + \mathbf{u}_0 - \mathbf{G}(\mathbf{x}) \mathbf{u}_c \quad (\text{A4})$$

If $\hat{f}_i^*(\mathbf{x}) = \hat{f}_i(\mathbf{x}, \theta_{f_i}^*)$ and $\hat{g}_{ik}^*(\mathbf{x}) = \hat{g}_{ik}(\mathbf{x}, \theta_{g_{ik}}^*)$ for $i, k = 1, \dots, m$ then we can write:

$$\mathbf{F}(\mathbf{x}) - \hat{\mathbf{F}}(\mathbf{x}) = \hat{\mathbf{F}}^*(\mathbf{x}) - \hat{\mathbf{F}}(\mathbf{x}) + \boldsymbol{\varepsilon}_f(\mathbf{x}) \quad (\text{A5})$$

$$\mathbf{G}(\mathbf{x}) - \hat{\mathbf{G}}(\mathbf{x}) = \hat{\mathbf{G}}^*(\mathbf{x}) - \hat{\mathbf{G}}(\mathbf{x}) + \boldsymbol{\varepsilon}_g(\mathbf{x}) \quad (\text{A6})$$

Substituting (A5) and (A6) into (A4), we have

$$\begin{aligned} \dot{\mathbf{s}} = & -\mathbf{K}_0 \mathbf{s} - \mathbf{K}_1 \text{sgn}(\mathbf{s}) - (\hat{\mathbf{F}}^*(\mathbf{x}) - \hat{\mathbf{F}}(\mathbf{x})) \\ & - (\hat{\mathbf{G}}^*(\mathbf{x}) - \hat{\mathbf{G}}(\mathbf{x})) \mathbf{u}_{eq} + \mathbf{u}_0 \\ & - \mathbf{G}(\mathbf{x}) \mathbf{u}_c - \boldsymbol{\varepsilon}_f(\mathbf{x}) - \boldsymbol{\varepsilon}_g(\mathbf{x}) \mathbf{u}_{eq} \end{aligned} \quad (\text{A7})$$

Multiplying \mathbf{s}^T to (A7) gives

$$\begin{aligned} \mathbf{s}^T \dot{\mathbf{s}} = & -\mathbf{s}^T \mathbf{K}_0 \mathbf{s} - \mathbf{s}^T \mathbf{K}_1 \text{sgn}(\mathbf{s}) - \sum_{i=1}^m \psi_{f_i}^T \tilde{\theta}_{f_i} s_i \\ & - \sum_{i=1}^m \sum_{k=1}^m \psi_{g_{ik}}^T \tilde{\theta}_{g_{ik}} s_i u_{eqk} + \mathbf{s}^T \mathbf{u}_0 \\ & - \mathbf{s}^T \mathbf{G}(\mathbf{x}) \mathbf{u}_c - \mathbf{s}^T \boldsymbol{\varepsilon}_f(\mathbf{x}) - \mathbf{s}^T \boldsymbol{\varepsilon}_g(\mathbf{x}) \mathbf{u}_{eq} \end{aligned} \quad (\text{A8})$$

where $\tilde{\theta}_{f_i} = \theta_{f_i}^* - \theta_{f_i}$, $\tilde{\theta}_{g_{ik}} = \theta_{g_{ik}}^* - \theta_{g_{ik}}$

Apply (A8) to (A2), we have

$$\dot{V} = -\mathbf{s}^T \mathbf{K}_0 \mathbf{s} - \mathbf{s}^T \mathbf{K}_1 \text{sgn}(\mathbf{s}) + \dot{V}_1 + \dot{V}_2 \quad (\text{A9})$$

where

$$\dot{V}_1 = - \sum_{i=1}^m \tilde{\theta}_{f_i}^T (\psi_{f_i}(\mathbf{x}) s_i + \frac{1}{\eta_{f_i}} \dot{\theta}_{f_i}) \quad (\text{A10})$$

$$- \sum_{i=1}^m \sum_{k=1}^m \tilde{\theta}_{g_{ik}}^T (\psi_{g_{ik}}(\mathbf{x}) s_i u_{eq} + \frac{1}{\eta_{g_{ik}}} \dot{\theta}_{g_{ik}})$$

$$\dot{V}_2 = -\mathbf{s}^T \mathbf{G}(\mathbf{x}) \mathbf{u}_c + \mathbf{s}^T \mathbf{u}_0 - \mathbf{s}^T \boldsymbol{\varepsilon}_f(\mathbf{x}) - \mathbf{s}^T \boldsymbol{\varepsilon}_g(\mathbf{x}) \mathbf{u}_{eq} \quad (\text{A11})$$

Substituting the parameter adaptation laws (20) and (21) into (A10) gives

$$\dot{V}_1 = 0 \quad (\text{A12})$$

From Assumption 1, we can write

$$\mathbf{s}^T \mathbf{G}(\mathbf{x}) \mathbf{s} \geq \delta_0 \|\mathbf{s}\|^2 \quad (\text{A13})$$

Multiplying $\frac{|\mathbf{s}^T (\bar{\varepsilon}_f + \bar{\varepsilon}_g \mathbf{u}_{eq}) + \mathbf{u}_0|}{\delta_0 \|\mathbf{s}\|^2}$ to (A13) gives

$$\mathbf{s}^T \mathbf{G}(\mathbf{x}) \mathbf{s} \frac{|\mathbf{s}^T (\bar{\varepsilon}_f + \bar{\varepsilon}_g \mathbf{u}_{eq}) + \mathbf{u}_0|}{\delta_0 \|\mathbf{s}\|^2} \geq |\mathbf{s}^T (\bar{\varepsilon}_f + \bar{\varepsilon}_g \mathbf{u}_{eq}) + \mathbf{u}_0| \quad (\text{A14})$$

Then

$$\mathbf{s}^T \mathbf{G}(\mathbf{x}) \mathbf{u}_c \geq |\mathbf{s}^T (\bar{\varepsilon}_f + \bar{\varepsilon}_g \mathbf{u}_{eq}) + \mathbf{u}_0| \quad (\text{A15})$$

From (A11) and (A15),

$$\dot{V}_2 \leq 0 \quad (\text{A16})$$

Substituting (A16) into (A9) leads to

$$\dot{V} \leq -\mathbf{s}^T \mathbf{K}_0 \mathbf{s} - \mathbf{s}^T \mathbf{K}_1 \text{sgn}(\mathbf{s}) \quad (\text{A17})$$

By using Barbalat's lemma in [33], (A17) implies $s \rightarrow 0$ as $t \rightarrow \infty$. This completes the proof.

REFERENCES

- [1] M. R. Popović, T. Keller, I. P. Pappas, V. Dietz, and M. Morari, "Surface-stimulation technology for grasping and walking neuroprostheses," *IEEE Eng. Med. Biol. Mag.*, vol. 20, no. 1, pp. 82-93, 2001.
- [2] J. J. Abbas and H. J. Chizeck, "Feedback control of coronal plane hip angle in paraplegic subjects using functional neuromuscular stimulation," *IEEE Trans. Biomed. Eng.*, vol. 38, no. 7, pp. 687-698, Jul. 1991.
- [3] N. Lan, P. E. Crago, and H. J. Chizeck, "Control of end-point forces of a multi-joint limb by functional electrical stimulation," *IEEE Trans. Biomed. Eng.*, vol. 38, no. 10, pp. 935-965, Oct. 1991.
- [4] L. A. Bernotas, P. E. Crago, and H. J. Chizeck, "Adaptive control of electrically stimulated muscle," *IEEE Trans. Biomed. Eng.*, vol. 34, no.2, pp. 140-147, Feb. 1987.
- [5] M. S. Hatwell, B. J. Oderkerk, C. A. Sacher, and G. F. Inbar, "The development of a model reference adaptive controller to control the knee joint of paraplegics," *IEEE Trans. Automat. Contr.*, vol. 36, no. 6, pp. 683-691, Jun. 1991.
- [6] N. Lan, P. E. Crago, and H. J. Chizeck, "Feedback control methods for task regulation by electrical stimulation of muscle," *IEEE Trans. Biomed. Eng.*, vol. 38, no. 12, pp. 1213-1223, Dec. 1991.
- [7] F. Previdi and E. Carpanzano, "Design of a gain scheduling controller for knee-joint angle control by using functional electrical stimulation," *IEEE Trans. Contr. Syst. Technol.*, vol. 11, no.3, pp. 310-324, May 2003.
- [8] G.-C. Chang, J.-J. Luh, G.-D. Liao, J.-S. Lai, C.-K. Cheng, B.-L. Kuo, and T.-S. Kuo, "A neuro-control system for the knee joint position control with quadriceps stimulation," *IEEE Trans. Rehabil. Eng.*, vol. 5, no.1, pp. 2-11, Mar. 1997.
- [9] M. Ferrarin, F. Palazzo, R. Riener, and J. Quintern, "Model based control of FES-induced single joint movements," *IEEE Trans. Neural Syst. Rehabil. Eng.*, vol. 9, no.3, pp. 245-257, Sept. 2001.
- [10] J. J. Abbas and H. J. Chizeck, "Neural network control of functional neuromuscular stimulation systems: computer simulation studies," *IEEE Trans. Biomed. Eng.*, vol. 42, no. 11, pp. 1117-1127, Nov. 1995.
- [11] J. J. Abbas and R. J. Triolo, "Experimental evaluation of an adaptive feedforward controller for use in functional neuromuscular stimulation systems," *IEEE Trans. Rehabil. Eng.*, vol. 5, no. 1, pp. 12-22, Mar. 1997.
- [12] J. Riess and J. J. Abbas, "Adaptive neural network control of cyclic movements using functional neuromuscular stimulation," *IEEE Trans. Rehabil. Eng.*, vol. 8, no. 1, pp. 42-52, Mar. 2000.
- [13] J. Riess and J. J. Abbas, "Adaptive control of cyclic movements as muscles fatigue using functional neuromuscular stimulation," *IEEE Trans. Neural Syst. Rehabil. Eng.*, vol. 9, no. 3, pp. 326-330, Sep. 2001.
- [14] R. Mirizarandi, A. Erfanian, and H. R. Kobravi, "Adaptive inverse control of knee joint position in paraplegic subjects using recurrent neural network," presented at the 10th Annu. Conf. Int. Functional Electr. Stimul. Soc., Montreal, QC, Canada, 2005.
- [15] K. Kurosawa, R. Futami, T. Watanabe, and N. Hoshimiya, "Joint angle control by FES using a feedback error learning controller," *IEEE Trans. Neural Syst. Rehabil. Eng.*, vol. 13, no.3, pp. 359-371, Sept. 2005.
- [16] D. B. Popović, R. B. Stein, M. N. Oğuztöreli, M. Lebedowska, and S. Jonić, "Optimal control of walking with functional electrical stimulation: A computer simulation study," *IEEE Trans. Rehab. Eng.*, vol. 7, no. 1, pp. 69-79, Mar. 1999.
- [17] F. C. Anderson and M. G. Pandy, "Dynamic optimization of human walking," *J. Biomech. Eng.*, vol. 123, no. 5, pp. 381-390, 2001.
- [18] D. G. Thelen and F. C. Anderson, "Using computed muscle control to generate forward dynamic simulations of human walking from experimental data," *J. Biomech.*, vol. 39, no. 6, pp. 1107-1115, 2006.
- [19] P.A. Ioannou and J. Sun, *Robust Adaptive Control*. PTR Prentice-Hall, Englewood Cliffs, 1996.
- [20] D. Hongliu and S.S. Nair, "Learning control design for a class of nonlinear systems," *Engineering Applications of Artificial Intelligence*, vol. 11, no.4, pp. 495-505, Aug. 1998.
- [21] T. Zhang, S. S. Ge, C. C. Hang, and T. Y. Chai, "Adaptive control of first-order systems with nonlinear parameterization," *IEEE Trans. Automat. Contr.*, vol. 45, no. 8, pp. 1512-1516, Aug. 2000.
- [22] Daniel E. Miller, "A new approach to model reference adaptive control," *IEEE Trans. Automat. Contr.*, vol. 48, no. 5, pp. 743-757, May 2003.
- [23] J.-J. E. Slotine and W. Li, *Applied Nonlinear Control*. NJ: Prentice Hall, 1991.
- [24] K. D. Young, V. Utkin, and Ü. Özgüner, "A control engineer's guide to sliding mode control," *IEEE Trans, Contr. Syst. Technol*, vol. 7, no. 3, pp. 328-342, May 1999.
- [25] J. Guldner and V. Utkin, "The chattering problem in sliding mode systems," Proc. 14th Int. Symposium of Mathematical Theory of Networks and Systems, MTNS, Perpignan, France, 2000.
- [26] Ajoudani and A. Erfanian, "A neuro-sliding mode control with adaptive modeling of uncertainty for control of movement in paralyzed limbs using functional electrical stimulation," *IEEE Trans. Biomed. Eng.*, vol. 56, pp. 1771-1780, Jul. 2009.
- [27] H. R. Kobravi and A. Erfanian, "Decentralized adaptive robust control based on sliding mode and nonlinear compensator for the control of ankle movement using functional electrical stimulation of agonist-antagonist muscles," *J. Neural Eng.*, vol.6, pp. 1-10, 2009.
- [28] L.-X. Wang, *Adaptive Fuzzy Systems and Control*:

- Design and Stability Analysis*. Prentice-Hall, NJ: Englewood Cliffs, 1994.
- [29] J. Wang, A.B. Rad, and P.T. Chan, "Indirect adaptive fuzzy sliding mode control: Part I: fuzzy switching," *Fuzzy Sets Syst.*, vol. 122, pp. 21-30, 2001.
- [30] J.-P. Su, T.-M. Chen, and C.-C. Wang, "Adaptive fuzzy sliding mode control with GA-based reaching laws," *Fuzzy Sets Syst.*, vol. 120, pp. 145-158, 2001.
- [31] S. Labiod, and T.-M. Guerra, "Indirect adaptive fuzzy control for a class of nonaffine nonlinear systems with unknown control directions," *Int. J. Contr. Automat. Syst.*, vol. 8, no. 4, pp. 903-907, 2010.
- [32] H. Layeghi, M. T. Arjmand, H. Salarieh, and A. Alasty, "Stabilizing periodic orbits of chaotic systems using fuzzy adaptive sliding mode control," *Chaos Solutions and Fractals*, vol. 37, pp. 1125-1135, 2008.
- [33] C.-M. Lin and Y.-J. Mon, "Decoupling control by hierarchical fuzzy sliding-mode controller," *IEEE Trans. Contr. Syst. Technol.*, vol. 13, no. 4, pp. 593-598, Jul. 2005.
- [34] T.-P. Zhang, "Stable adaptive fuzzy sliding mode control of interconnected systems," *Fuzzy Sets Syst.*, vol. 122, no. 1, pp. 5-19, Aug. 2001.
- [35] Y.-C. Hsu, G. Chen, and H.-X. Li, "A fuzzy adaptive variable structure controller with applications to robot manipulators," *IEEE Trans. Syst., Man, Cybern. B, Cybern.*, vol. 31, no. 3, pp. 331-340, Jun. 2001.
- [36] F. Zheng, Q.-G. Wang and Tong Heng Lee, "Output tracking control of MIMO fuzzy nonlinear systems using variable structure control approach," *IEEE Trans. Fuzzy Syst.*, vol. 10, no. 6, pp. 686-697, Dec. 2002.
- [37] S. Tong and H.-X. Li, "Fuzzy adaptive sliding-mode control for MIMO nonlinear systems," *IEEE Trans. Fuzzy Syst.*, vol. 11, no. 3, pp. 354-360, Jun. 2003.
- [38] Y. Guo and P.-Y. Woo, "An adaptive fuzzy sliding mode controller for robotic manipulators," *IEEE Trans. Syst., Man, Cybern. A, Syst. Humans*, vol. 33, no.2, pp. 149-159, Mar. 2003.
- [39] C.-L. Hwang, "A novel Takagi-Sugeno-based robust adaptive fuzzy sliding-mode controller," *IEEE Trans. Fuzzy Syst.*, vol. 12, no. 5, pp. 676-687, Oct. 2004.
- [40] S. Labioda, M. S. Boucherith, and T. M. Guerrac, "Adaptive fuzzy control of a class of MIMO nonlinear systems," *Fuzzy Sets Syst.*, vol. 151, pp. 59-77, 2005.
- [41] X.-Y. Lu and S. K. Spurgeon, "Robust sliding mode control of uncertain nonlinear systems," *Syst. Contr. Letters*, vol. 32, pp. 75-90, 1997.
- [42] S. Došen and D. B. Popović, "Moving-window dynamic optimization: design of stimulation profiles for walking," *IEEE Trans. Biomed. Eng.*, vol. 56, no. 5, pp. 1298-1309, May. 2009.
- [43] G. I. Zahalak, J. M. Winters, and S. L. Y. Woo, *Multiple Muscle Systems: Biomechanics and Movement Organisation*. NY: Springer Verlag; 1990.
- [44] G. T. Yamaguchi and F. E. Zajac, "Restoring unassisted natural gait to paraplegics via functional neuromuscular stimulation: a computer simulation study," *IEEE Trans Biomed. Eng.*, vol. 37, no. 9, pp. 886-902, Sep. 1990.
- [45] Erfanian, H. R. Kobravi, O. Zohorian, and F. Emani, "A portable programmable transcutaneous neuroprosthesis with built-in self-test capability for training and mobility in paraplegic subjects," Proc. 11th Ann. Conf. Int. Functional Electrical Stimulation Society, 2006.
- [46] D. A. Winter, *Biomechanics and Motor Control of Human Movement*. NY: Wiley, 1990.



Vahab Nekoukar received the B.S. and M.Sc. degree in Electrical Engineering from Khaje Nasir Toosi University in 2005 and Tarbiat Modares University in 2007, respectively. He is currently candidate of Ph.D. in Electrical Engineering in INTRC, Iran University of Science and Technology. His research interests include adaptive and nonlinear control and control of neuromusculoskeletal systems.



Abbas Erfanian received the B.S. degree in computer engineering from Shiraz University, Shiraz, in 1985, the M.S. degree in computer engineering from Sharif University of Technology, Tehran, in 1989, the Ph. D. degree in biomedical engineering from Tarbiat Modarres University, Tehran, Iran in 1995.

In 1993 he was a Senior Research Associate at Case Western Reserve University and VA Medical Center, Cleveland, OH, USA, where he did research in the area of functional electrical stimulation, and neuromuscular control systems. Since 1995, he has been a faculty member at Iran University of Science and Technology (IUST), in Tehran, IRAN, serving as Chair of Biomedical Engineering Group from 2000-2007. Currently he is an Associate Professor of Biomedical Engineering at the IUST.

His research interests are artificial neural network, biomedical signal processing, neural engineering, chaos theory and its application to biomedical problems, Functional Electrical Stimulation, and brain-computer interface. Erfanian is a member of the International Functional Electrical Stimulation Society (IFESS), IEEE, and the IEEE Engineering in Medicine and Biology Society (IEEE-EMBS).